

ON ACCURACY OF NUMERICAL SOLUTION TO BOUNDARY VALUE PROBLEMS ON INFINITE DOMAINS WITH SLOW DECAY

KYLE BOOKER¹ AND YANA NEC¹

Abstract. A numerical approach is developed to solve differential equations on an infinite domain, when the solution is known to possess a slowly decaying tail. An unorthodox boundary condition relying on the existence of an asymptotic relation for $|y| \gg 1$ is implemented, followed by an optimisation procedure, allowing to obtain an accurate solution over a truncated finite domain. The method is applied to $-(-\Delta)^{\gamma/2}u - u + u^p = 0$ in \mathbb{R} , a non-linear integro-differential equation containing the fractional Laplacian, and is easily expanded to asymmetric boundary conditions or domains of a higher dimension.

Mathematics Subject Classification. 45K05, 37M99.

The dates will be set by the publisher.

INTRODUCTION

The numerical approach developed herein is suitable for a differential equation of any type on an infinite domain, bar perhaps a singular perturbation, provided an asymptotic approximation exists for each slowly decaying tail. To introduce the method and report accuracy results thereon, it is chosen to focus on a particular equation of substantial complexity that involves the fractional Laplacian and a non-linear source. Therefore an overview is in order on the challenges associated with fractional operators as well as this specific equation.

Differential operators of an arbitrary order, historically named fractional, are a generalisation of the common integer order operators [19]. Numerous applications require these operators to model transport processes that cannot be faithfully described by integer order differential equations [13, 20]. The complexity of fractional operators is such that advances in pure theory as well as analytical insight into specific problems are relatively scarce and far between [1, 4, 8]. Often the crux is the failure of fractional derivatives to satisfy basic properties expected from a derivative. Thus whilst an integer derivative is a single undisputed notion, there are many types of fractional ones adapted for different purposes. Classical definitions include the Grünwald-Letnikov generalisation of the Riemann sum, its continuum equivalent the Riemann-Liouville integral and a particular case thereof with an infinite lower integration bound, the Weyl derivative [19]. The first is best known for giving proper limits at all integers, i.e. when the order tends to an integer, the corresponding integer operator is recovered. The second is the most convenient in analytical problems, nonetheless rarely tractable. Both operators possess no spectrum and the constant functions are not in the kernel. Some variants, where the kernel contains the constant functions, are Caputo and Elliot derivatives [7]. The Weyl derivative is the only fractional

Keywords and phrases. Slowly decaying tail, infinite domain, boundary value problem, fractional Laplacian, ground state solution

¹ Department of Mathematics and Statistics, Thompson Rivers University, Kamloops, British Columbia, Canada,
e-mail: cranberryana@gmail.com

one to possess a spectrum and is instrumental in forming the fractional Laplacian operator, whose kernel also contains the constant functions.

Numerical treatment of these operators has proven challenging on many levels. The fractional derivative is essentially a convolution integral with a singular kernel. Familiar discretisation techniques yield unintuitive accuracy and stability characteristics. An example of unexpected accuracy properties is the first order approximation of the Crank-Nicholson method due to the fractional operator solely, as compared to the second order for classical derivatives. For a space-fractional advection – dispersion equation both explicit and implicit Euler schemes and Crank-Nicholson scheme, based on Grünwald discrete formula for the fractional operator, are unconditionally unstable [17]. Moreover, grid refinement rendered the scheme inconsistent, i.e. the numerical solution did not converge to the exact one. To resolve the problem an optimal for that equation shifting of the Grünwald formula was found to yield a consistent and stable scheme. Another interesting example is an asymmetric discretisation of the fractional operator giving more accurate results, when the operator order parameter was far enough from the value corresponding to the non-fractional equation [16]. The important inference of these studies is that a fractional equation is likely to require a custom treatment.

Fractional equations over infinite domains are a wide class of equations, whose solutions are known to exhibit slowly decaying tails, e.g. algebraic or logarithmic [22]. These might emerge not only when the natural domain associated with a problem is infinite, but for instance as an inner solution in a matched asymptotic expansions approach [18]. An immediate concern is the application of boundary conditions at infinity and domain truncation. For example, fronts [6, 23] or spikes [18] with Lévy flights as the underpinning diffusion mechanism, are produced by equations containing $-(\Delta)^{\gamma/2}$, $1 \leq \gamma < 2$, and have algebraic tails decaying as $|y|^{-(\gamma+1)}$. When $\gamma = 2$, the operator is the regular Laplacian and the tail decay is exponential. Both the front and spike solutions have a very narrow region of interest, where most of the changes in function value and gradient are located. However, with $\gamma = 2$ a domain length of 20 results in function value on the order $\mathcal{O}(10^{-9})$, whereas for $\gamma = 1.5$ it is $\mathcal{O}(10^{-2})$. This simple calculation calls forth the inference that applying a Dirichlet or Neumann boundary condition at the end points of the interval will entail a solution with a grossly distorted tail and is bound to affect the core region of interest. Some of these effects were studied in [6]. Although numerous equations involving the fractional Laplacian or operators of equivalent complexity have been solved numerically with different degrees of success, from linear [14, 15] to non-linear [18], virtually no results are reported on the possible distortion due to misapplied boundary conditions. In [18] the questionable accuracy of the numerical solution due to the slow tail decay was mentioned, but not duly analysed.

Fronts decay as $|y|^{-\gamma}$, the estimate is for that.

The numerical error unwittingly introduced due to a truncated domain might exceed by several orders of magnitude the error guaranteed by the solution scheme itself, when the solution decay at infinity is too slow to perform the computation on a sufficiently large domain. The proposed method to control the error is applied to the example equation

$$\mathfrak{D}_{|y|}^{\gamma} u - u + u^p = 0, \quad 1 < \gamma < 2, \quad (1a)$$

with the conditions

$$u(\pm\infty) = 0, \quad u(y) > 0, \quad u(y) = u(-y). \quad (1b)$$

The non-linearity parameter p satisfies $p > 1$. The integer order counterpart of (1a) is

$$u'' - u + u^p = 0 \quad (1c)$$

with the same boundary conditions. The operator $\mathfrak{D}_{|y|}^{\gamma}$ is the fractional Laplacian in one dimension

$$\mathfrak{D}_{|y|}^{\gamma} f(y) = -\frac{\sec(\pi\gamma/2)}{2\Gamma(2-\gamma)} \frac{d^2}{dy^2} \left\{ \int_{-\infty}^y \frac{f(\xi) d\xi}{(y-\xi)^{\gamma-1}} + \int_y^{\infty} \frac{f(\xi) d\xi}{(\xi-y)^{\gamma-1}} \right\} = \frac{\sec(\pi\gamma/2)}{2\Gamma(-\gamma)} \int_{-\infty}^{\infty} \frac{f(y) - f(\xi)}{|y-\xi|^{\gamma+1}} d\xi, \quad (2a)$$

or for Fourier transformable functions defined for any $\mathbf{y} \in \mathbb{R}^n$ as

$$\mathcal{F}_{\mathbf{y} \rightarrow q} \left\{ -(-\Delta)^{\gamma/2} f(\mathbf{y}) \right\} = -|\mathbf{q}|^\gamma \mathcal{F}_{\mathbf{y} \rightarrow q} \{ f(\mathbf{y}) \}, \quad 1 \leq \gamma \leq 2. \quad (2b)$$

The first equality in (2a) is a sum of two Weyl derivatives, whereas the second integral makes it obvious the constant functions are in the kernel of this operator.

Equation (1a) attracts a general interest and belongs to a wide class of investigated fundamental non-linear problems [3, 5, 9, 21], but also surfaces as an auxiliary equation in specific problems such as the Gierer-Meinhardt system, where it represents a localised reactant concentration – a spike [18]. For brevity hereunder the solution to (1) will be referred to as such. The existence, uniqueness and boundedness of solutions to (1a) as a generalisation of (1c) has been studied for quite some time in more than one spatial dimension and for parameters (p, γ) in a wider range than required for specific problems, cf. the seminal work [8] and references therein. The solution to (1c) is known in closed form for all p :

$$u(y) = \left\{ \frac{p+1}{2} \operatorname{sech}^2 \left(\frac{p-1}{2} y \right) \right\}^{1/(p-1)}, \quad (3a)$$

however for (1a) only one exact solution is available for $(p, \gamma) = (2, 1)$:

$$u(y) = \frac{2}{1+y^2}. \quad (3b)$$

The tail in (3a) decays exponentially, whilst in (3b) the decay is algebraic. In a phase plane the orbit (3a) is a homoclinic, whereas (3b) is referred to as a ground state solution. In [18] it is proved that

$$u(y) \sim a(p, \gamma) y^{-(\gamma+1)} \quad \forall 1 \leq \gamma < 2. \quad (4)$$

Thence it follows that the limit $\gamma \rightarrow 2^-$ is improper: regardless of how close to 2 the anomaly index γ is, the tail will never approach an exponential decay and the function shape will not converge to (3a). On the other hand, the limit $\gamma \rightarrow 1^+$ is proper, whereby (3b) can gauge the capability of different numerical schemes.

A numerical solution of (1a) was attempted in [18] with only partial success due to the aforementioned error source. With $\gamma = 2$ it is sufficient to prescribe $u = 0$ at the end points, because the tail decay is exponential. However, a similar application for an algebraically decaying tail cannot work well, since for no reasonable interval will the tail decay close to machine zero at the ends. The proposed mending of the tail discretising $u'(y) \sim -(\gamma+1)u(y)/y$ based on the asymptotic relation (4) met with difficulties. One, implementing this only at the last two (first order) or three (second order) points yielded unviable solutions. An untraditional implementation over a significantly larger part of the tail improved the result, yet the error magnitude could not be estimated, because it was unclear how to determine the portion of the tail, where this condition would be implemented. In particular, because $u' < 0 \forall y > 0$, the values of u at the tail would become negative if the mending point was too close to the spike centre, whereas non-smooth profiles ensued if it was not close enough. Moreover, counter-intuitively the error was exacerbated for γ values in the range $1.75 \lesssim \gamma < 2$, where the tail decay is in fact faster. Clearly a sound error control scheme is required in order to obtain a trustworthy solution, regardless of the actual numerical scheme being used.

To summarise, in boundary value problems with slowly decaying functions on infinite domains a significant error is introduced when traditional boundary conditions are implemented, regardless of the numerical solution scheme in use. The distortion diffuses into the domain and affects even solutions, whose region of interest is relatively narrow. A visual example of the extent of this phenomenon is given in figure 1. The current contribution offers a generic method to control this error source.

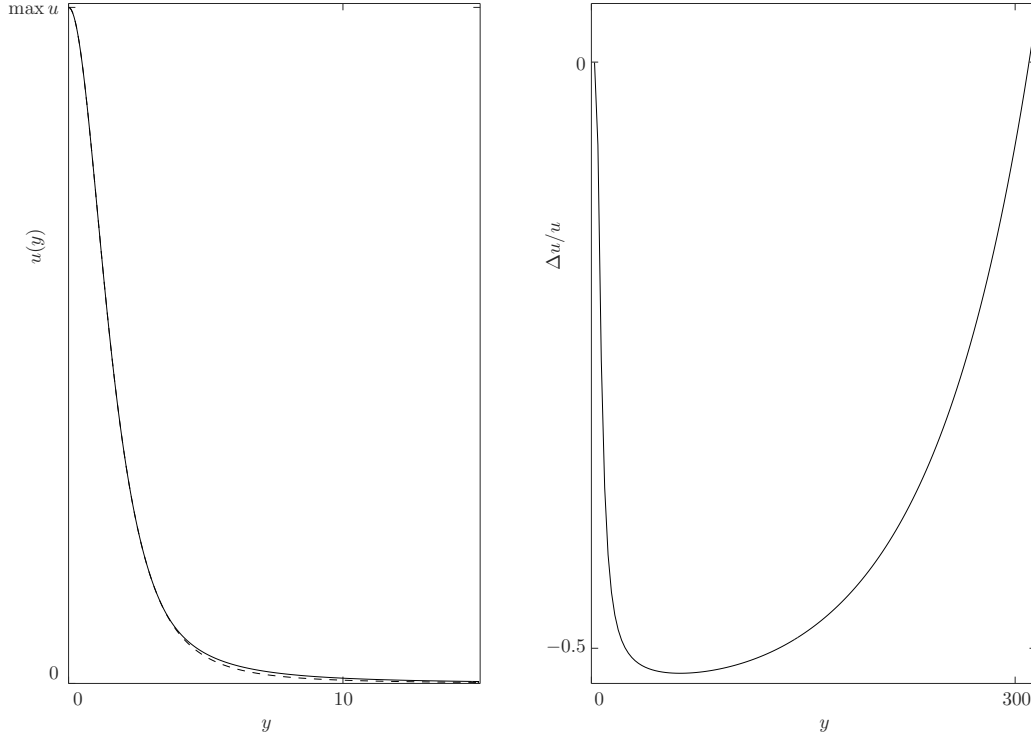


FIGURE 1. Spike solution with (solid) and without (dashed) tail error control for $p = 2$ and $\gamma = 1.5$ (left) and relative error of the two (right). $u(-y) = u(y)$.

1. TAIL CONDITIONS

The core numerical scheme is briefly outlined here for convenience and the reader is referred to [18] for further technical detail. At the limit $\epsilon \rightarrow 0$ and $D \rightarrow \infty$ the system

$$\mathbf{u}_t = \epsilon^\gamma \mathfrak{D}_{|y|}^\gamma \mathbf{u} - \mathbf{u} + \frac{\mathbf{u}^p}{\mathbf{v}}, \quad (5a)$$

$$\tau_o \mathbf{v}_t = D \mathbf{v}_{yy} - \mathbf{v} + \frac{\mathbf{u}^p}{\epsilon}, \quad (5b)$$

possesses a steady state that is the sought solution to (1a). Relying on (2b) simplifies the numerical treatment of the fractional Laplacian operator, circumventing two main issues: kernel singularity and truncation of the infinite integration domain. Thus the system

$$\frac{d\hat{\mathbf{u}}}{dt} = -(\epsilon^\gamma |q|^\gamma + 1)\hat{\mathbf{u}} + \mathcal{F}\left\{\frac{\mathbf{u}^p}{\mathbf{v}}\right\}, \quad (6a)$$

$$\tau_o \frac{d\hat{\mathbf{v}}}{dt} = -(Dq^2 + 1)\hat{\mathbf{v}} + \mathcal{F}\left\{\frac{\mathbf{u}^p}{\epsilon}\right\}, \quad (6b)$$

where the hats denote Fourier transformed quantities, is integrated in time using the Euler scheme, with the linear and non-linear terms discretised by the Crank-Nicolson and Adams-Bashforth methods respectively. The

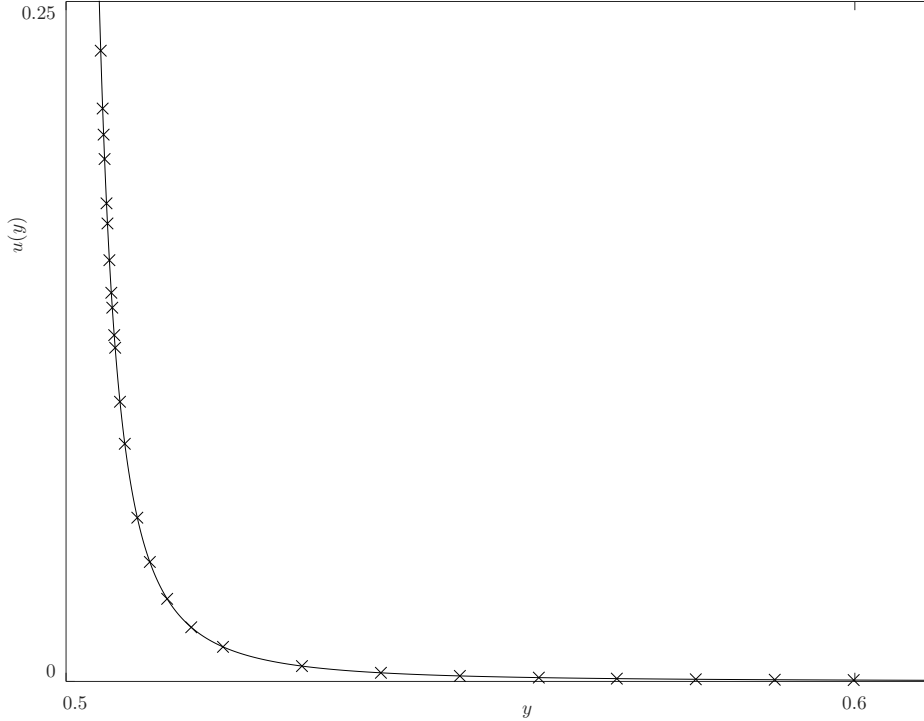


FIGURE 2. Tail condition implementation points marked on the tail of the ground state solution for $p = 2$, $\gamma = 1$. Abscissa scale shown as a fraction out of N , the number of mesh points and Fourier wavelengths.

initial condition is an interpolation of (3a) and (3b) for the relevant (p, γ) pair. Due to the slow decay of the sought function at infinity, the classic boundary condition on a truncated domain must be replaced with a tail condition. Such a replacement requires painstaking analysis. The two possibilities considered are discussed hereinafter.

1.1. Tail condition based on u and u'

The asymptotic relation (based on (4))

$$u' \sim -(\gamma + 1) \frac{u}{y} \quad y \rightarrow \infty \quad (7a)$$

was discretised to first order using the forward difference operator

$$u(x_{j+1}) = u(x_j) \left(1 - \frac{\gamma + 1}{j - N/2} \right) \quad (7b)$$

and second order with backward difference

$$u(x_{j+2}) = \frac{2u(x_{j+1}) - u(x_j)/2}{3/2 + (\gamma + 1)/(j - N/2)}, \quad (7c)$$

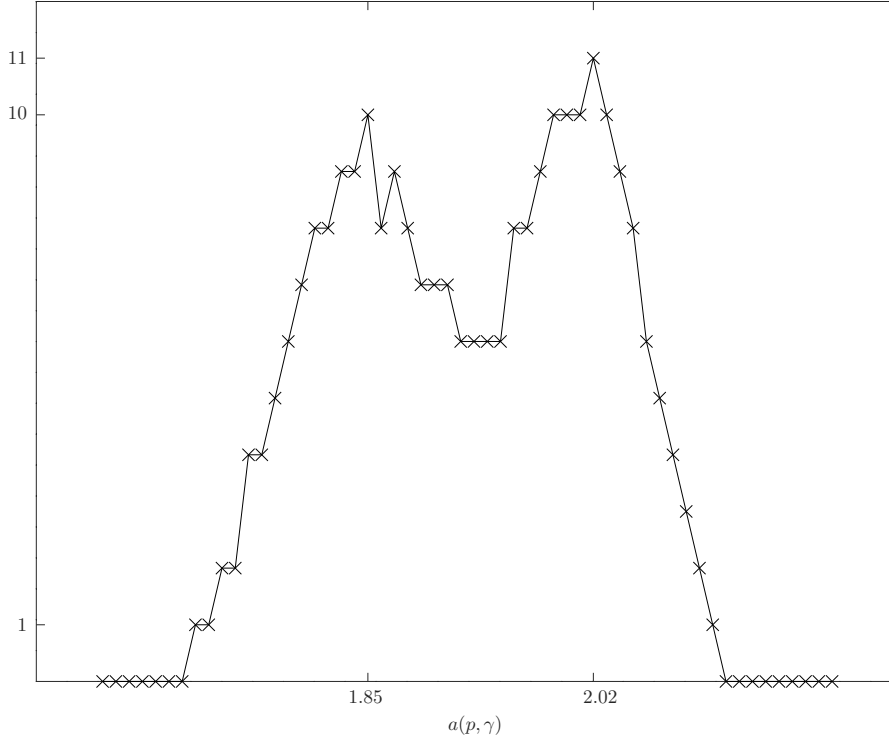


FIGURE 3. Sliding window histogram of raw values of $a(p, \gamma)$ for $p = 2$, $\gamma = 1$ and tail condition implementation points as in figure 2.

where N is the number of mesh points as well as wavelengths in the Fourier transform. Equation (4) implies that $\ln u$ is linear for $y \gg 1$, but there is no analytical way to determine $a(p; \gamma)$. Part of the problem is that for any sensible set of parameters $\epsilon \ll 1$, $D \gg 1$, τ_o and N the linearity is always recovered, however the value $a(p; \gamma)$ varies significantly. Relying on the exact solution (3b), both schemes were tested to seek a sound way to determine the point, where the tail condition must be implemented. Common numerical integration parameters are listed in appendix A. Scheme (7c) did not improve the overall accuracy attained. Hence, unless expressly stated, the results below refer to (7b).

The working assumption was that the correct solution would not be sensitive to the numerical scheme parameters and result in a smooth dependence $a(p, \gamma)$. To this end a sliding window histogram of the obtained $a(p, \gamma)$ values was constructed. Figures 2 and 3 depict a typical set of tail condition points and corresponding histogram. For this example problem the histogram is bimodal, and moreover the peaks are quite close in height, rendering the availability of an exact solution crucial. Starting with the known value $a(2, 1) = 2$, the correct peak is tracked as p and γ vary. If the numerical scheme yields a correct solution, the histogram peak evolution is gradual and $a(p, \gamma)$ is smooth in both arguments. Figure 3 also allows to infer the accuracy of $a(p, \gamma)$ as two significant digits. One must bear in mind that $a(p, \gamma)$ is a derived quantity (least squares fit to a straight line of $\ln u$), not a direct output of the numerical scheme with its expected discretisation error. In conjunction with the fractional Laplacian – as any singular integro-differential operator over an infinite domain – being the main source of error in this problem, the fact that the higher order tail scheme did not improve the accuracy of $a(p, \gamma)$ is not overly surprising. The finiteness of D and ϵ in system (5) also contributes error, since the sought ground

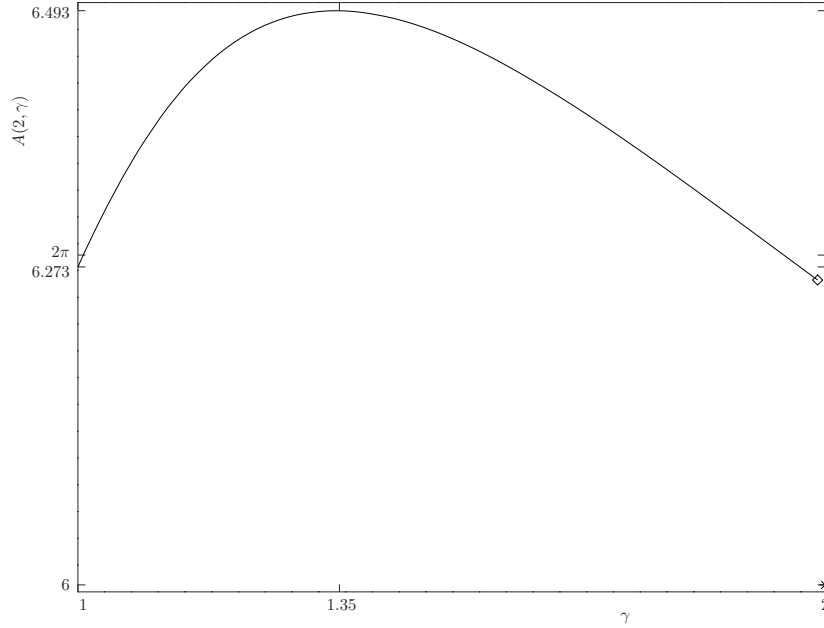


FIGURE 4. Area $A(p, \gamma) = \int_{-2\pi/\epsilon}^{2\pi/\epsilon} u(y; p, \gamma) dy$ for $p = 2$. Diamond marks the improper limit $\lim_{\gamma \rightarrow 2^-} A(p, \gamma)$, asterisk marks the value $A(p, 2)$.

state is a limit solution with $D \rightarrow \infty$ and $\epsilon \rightarrow 0$. Furthermore, since the effective domain is $|y| < 2\pi/\epsilon$, the errors due to the fractional Laplacian integral truncation and the finiteness of ϵ are interconnected. Figure 4 shows a quantitative measure of this error through the area under the obtained solutions. The worst error is expected for the slowest decaying function, i.e. $p = 2$ and $\gamma = 1$. The integral over \mathbb{R} of (3b) equals 2π (see also appendix B), whereas for $\epsilon = 0.01$ used in all computations

$$\int_{-2\pi/\epsilon}^{2\pi/\epsilon} \frac{2 dy}{1 + y^2} = 4 \arctan\left(\frac{2\pi}{\epsilon}\right) \approx 6.27682. \quad (8)$$

From figure 4 the numerically obtained value is 6.273 to three decimal places, whereby the error estimate is on the order of magnitude of 10^{-3} . Thus it will be consistent to deem $a(p; \gamma)$ accurate to second significant figure. An additional feature of interest in figure 4 is the improper limit $\gamma \rightarrow 2$. For $p = 2$, $\gamma = 2$ the integral over \mathbb{R} of (3a) equals 6 and is obtained to machine handling precision with the parameters in appendix A, whilst for $\gamma \rightarrow 2^-$ the diamond mark shows the limit just slightly under 2π value. The gap is therefore larger than the range of $A(p, \gamma) = \int_{-2\pi/\epsilon}^{2\pi/\epsilon} u(y; p, \gamma) dy$. This calculation quantifies the disparity between exponential and algebraic decay, substantiating the conundrum of implementing boundary conditions in the latter situation.

The optimal tail condition implementation point, to wit one yielding a correct numerical solution, is related to the comparative decay rate of an algebraic tail versus the exponential one. From a painstaking scrutiny of

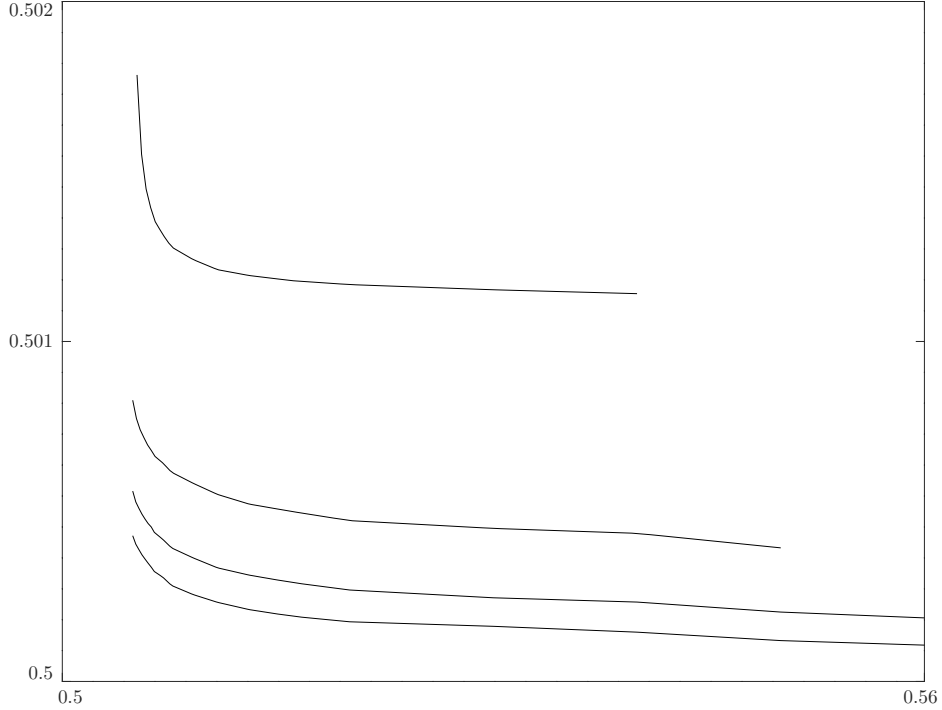


FIGURE 5. First positive root of $u(y; p, \gamma) - u(y; p, 2) = 0$ versus the correct tail condition implementation point for $p=2,3,4,5$ respectively from top curve to bottom. The anomaly index γ parameterises each curve right to left varying $1 \nearrow 2^-$.

overlaid ground states and the homoclinic (3a) in figures 7 and 8 the following intriguing observation is gleaned: the optimal point is directly related to the root to the equation $u(y; p, \gamma) - u(y; p, 2) = 0$. In fact there are two such roots in \mathbb{R}_+ , and the statement is correct with respect to either. Figure 5 depicts the typical dependence for several values of p . Note the functions are constant to the precision of two significant digits indicated for $a(p; \gamma)$.

1.2. Tail condition based on u , u' and u''

The asymptotic relation (4) was used to infer that

$$u'' + A \frac{u'}{y} + B \frac{u}{y^2} \sim 0, \quad B = (\gamma + 1)(A - \gamma - 2) \quad (9a)$$

and A an arbitrary constant of a commensurate order of magnitude. Since $u' < 0 \forall y > 0$, whereas $u > 0$ and $u'' > 0$, the inclusion of u'' was expected to aid in avoiding artificially negative values due to an overestimation of the tail decay rate. Discretising to first order using the forward difference operator yields

$$u(x_{j+2}) = u(x_{j+1}) \left(2 - \frac{A}{j - N/2} \right) - u(x_j) \left(1 - \frac{A}{j - N/2} + \frac{B}{(j - N/2)^2} \right), \quad (9b)$$

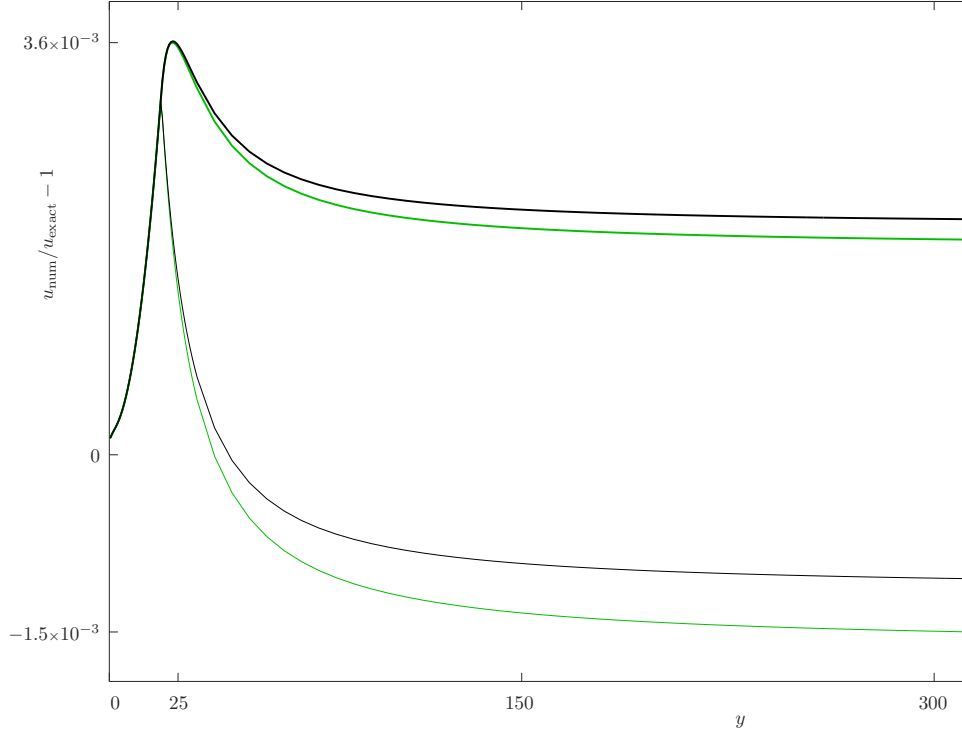


FIGURE 6. Relative error of numerical solutions with tail conditions based upon schemes (7b) (thin black), (7c) (thick black), (9b) (thin grey/green), (9c) (thick grey/green), and the true solution, equation (3b), for $p = 2$, $\gamma = 1$.

and similarly to second order with central difference

$$\mathbf{u}(x_{j+2}) = \frac{\mathbf{u}(x_{j+1}) \left(2 - B/(j - N/2)^2 \right) - \mathbf{u}(x_j) \left(1 - A/(2j - N) \right)}{1 + A/(2j - N)}. \quad (9c)$$

Here in addition to the analysis performed for the first derivative schemes (7), a range of values $1 \leq A \leq 50$ was tested, recovering the same results and thereby confirming the correctness of obtained ground state solutions for the entire range $1 \leq \gamma < 2$ and $2 \leq p \leq 5$.

A quantitative comparison of numerical solutions with the exact solution in the most extreme Lévy flights case for all foregoing schemes is given in figure 6. For this case the tail decay is the slowest, hence the error is the largest for any fixed p . As is seen from the error magnitude, all four tail discretisations yield similar accuracy. The error shape is typical for the developed approach: the error is minimal at the spike peak ($y = 0$), small and virtually constant at the tail ($y \gg 1$) and maximal in the vicinity of the point, where the tail condition is implemented. Amongst other things, this vindicates the introduction of the tail condition instead of a traditional boundary condition, as well as the significant part of the domain, where it must be applied. If the implementation interval is insufficient, the error continues to increase toward the boundaries of the domain due to premature or belated decay, begetting dearth of positivity, smoothness, monotonicity or any subset thereof. The reason second order schemes (7c) and (9c) are not markedly more accurate than the first order ones, (7b)

and (9b), stems from the fact the main source of error in this problem is the fractional Laplacian term in (1a) and concomitant Fourier forward and inverse transforms. Since the tail condition continues the obtained core solution, the tail accuracy is not given by the nominal scheme accuracy.

2. RESULTS

Figures 7 and 8 show the function $u(y; p, \gamma)$ for $p = 2$ and $p = 5$ respectively for representative values of γ in the range of Lévy flights $1 \leq \gamma < 2$. Interestingly, it is evident that near the core the slowest Lévy flights solution ($\gamma \rightarrow 2^-$, fractional Laplacian, highly non-local operator) would fall infinitesimally close to the regular homoclinic ($\gamma = 2$, simple Laplacian, local operator). Only at the tail the expected improper limit can be seen: the functions decay several orders of magnitude more slowly than the exponential. This is the feature that necessitates the special treatment of boundary conditions for these ground state solutions. The effect is much more pronounced for the higher values of p . Another point to observe is that as p increases, the intersection point of a Lévy flights ground state and the regular homoclinic shifts closer to $y = 0$. For this reason the tail condition implementation must begin earlier. The entire span of possible values is seen in figure 2.

Figure 9 shows the tail decay constant $a(p, \gamma)$ for the range $1 \leq \gamma < 2$ and integer values of $2 \leq p \leq 5$. The developed method yields smooth curves throughout the relevant range of γ . The limit $\gamma \rightarrow 2^-$ exists for each value of p , but never equals the value at $\gamma = 2$, which can be regarded as zero due to the exponential tail decay. As p increases for a fixed value of γ , the decay constant diminishes. Figure 10 gives a continuous variation versus p (in the original chemical model the non-linearity exponent must be integer, however this constraint can be relaxed in a purely mathematical setting) and representative values of γ . No local optima in p or γ were observed.

The maximal point of $u(y)$ is $u(0)$. The dependence of the maximal value on p and γ was unknown hitherto bar $\gamma = 2$ (equation (3a)) and the pair $(p, \gamma) = (2, 1)$ (equation (3b)). Figures 11 and 12 reveal monotonic decrease with γ or p for respectively fixed values of p or γ . It is interesting that both $a(p, \gamma)$ and $u(0; p, \gamma)$ exhibit monotonicity in both arguments. This is a non-trivial finding, as often generalisation of partial differential equations to fractional orders results in unexpected behaviour.

2.1. Validation of the tail constant

Continuity suggests that equation (4) can be re-written as

$$u(y) \sim u(y_*) \left(\frac{y}{y_*} \right)^{-(\gamma+1)}. \quad (10)$$

Thus if $u(y)$ was known, it would be possible to identify a point y_* such that the asymptotic relation (4) held to a prescribed error threshold in $a(p, \gamma)$, since $a(p, \gamma) = u(y_*)y_*^{\gamma+1}$ and for all $y > y_*$ this compound should remain invariant. Given that the accuracy of a numerically obtained solution $u(y)$ cannot be guaranteed to equal the scheme accuracy due to the reasons discussed in §1.1, equation (10) can be used either to confirm the correctness of the optimal value of $a(p, \gamma)$, or establish an iterative scheme to obtain it. This should be applicable to other problems, but might depend on the form of the asymptotic relation available. Figure 9 illustrates the concurrence of both methods for this example problem: the relative error is $\mathcal{O}(10^{-4})$ uniformly throughout the parameter space (p, γ) . The uniformity attests to the stability of the developed method in the sense that no error accumulation occurs when the optimisation procedure is applied to parameters pairs (p, γ) away from the control pair $(2, 1)$.

2.2. Non-linearity

Obtaining a single solution $u(y; p, \gamma)$ is quite expensive in both memory and computing time. This raises the question of non-linearity. In this case both the tail decay constant $a(p, \gamma)$ and the equation for $u(y; p, \gamma)$ are non-linear, however in a different problem the tail decay parameter(s) might be non-linear even if the equation

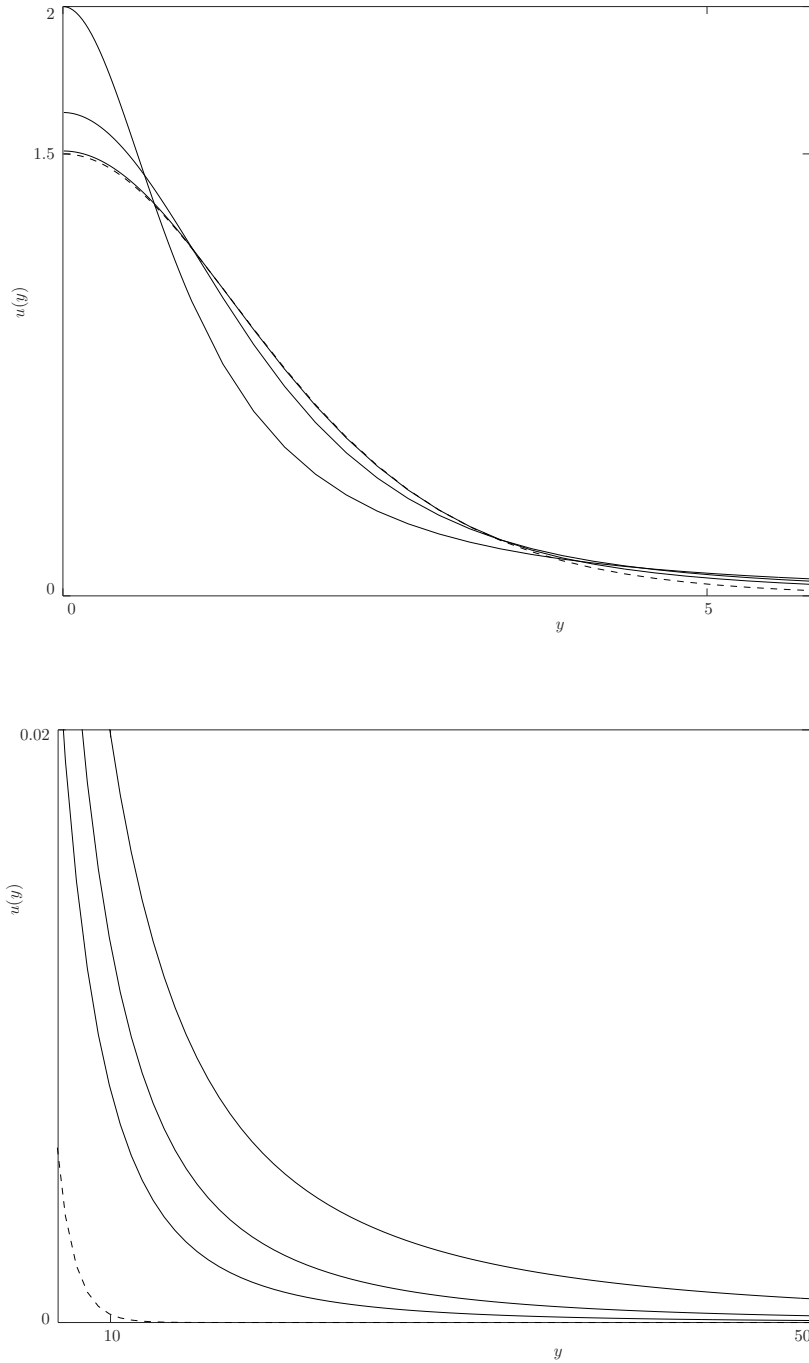


FIGURE 7. Solution $u(y; p, \gamma)$ for $p = 2$ and $\gamma = 1, 1.5, 1.95$ (Lévy flights, solid, respectively from top curve to bottom) and $\gamma = 2$ (regular diffusion, dashed). Upper panel: core, lower panel: tail. $u(-y) = u(y)$.

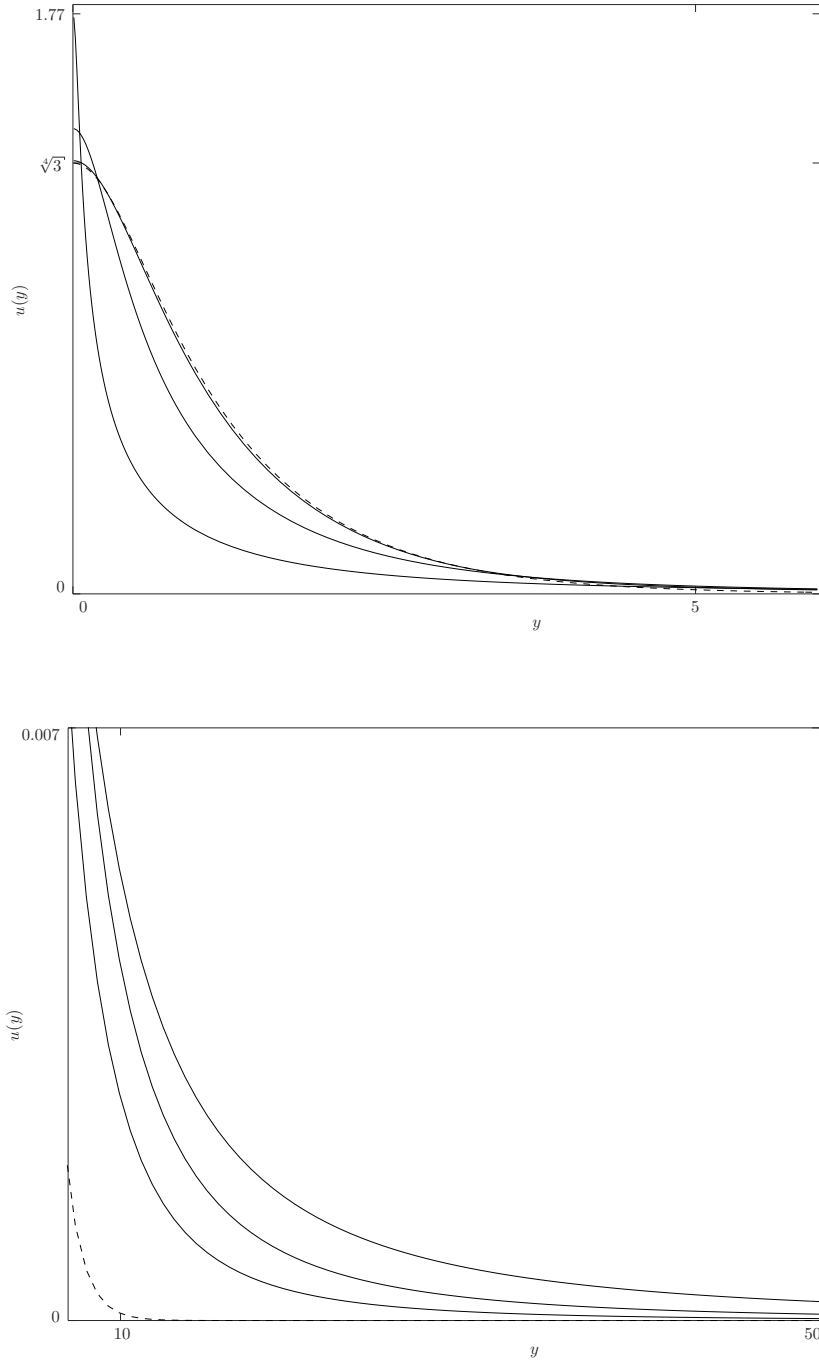


FIGURE 8. Solution $u(y; p, \gamma)$ for $p = 5$ and $\gamma = 1, 1.5, 1.95$ (Lévy flights, solid, respectively from top curve to bottom) and $\gamma = 2$ (regular diffusion, dashed). Upper panel: core, lower panel: tail. $u(-y) = u(y)$.

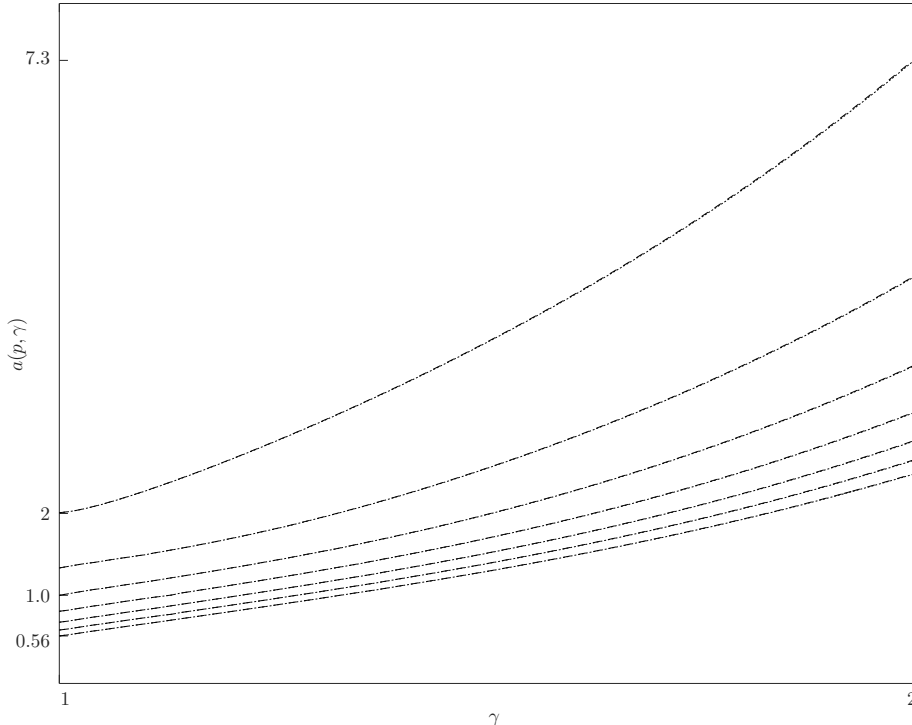


FIGURE 9. Tail constant $a(p, \gamma)$ for evenly spaced values $2 \leq p \leq 5$ in ascending order $2 \nearrow 5$ from top curve to bottom obtained by a linear fit of $\ln u$ (dashed, equation (4)) and mean of the invariant asymptotic (dotted, equation (10)).

itself is linear. Therefore in light of the error analysis in §1.1, care must be exercised. Could two sufficiently close solutions $u_i(y; p_i, \gamma_i)$, $i = \{1, 2\}$, be interpolated for any $\gamma_1 < \gamma < \gamma_2$ or $p_1 < p < p_2$ with a reasonable accuracy? The anomaly index γ in experimental studies is commonly estimated to the precision of two decimal places, cf. [2], whereas p is most often integer, although mathematically the problem is well posed for any $p > 1$.

Figures 13 and 14 illustrate the error incurred by interpolation in γ and p respectively versus a full numerical solution. In the former case the maximal relative error is always obtained at the tail and uniform in its order of magnitude throughout the parameter space, once more emphasising that obtaining an accurate solution in the tail region is highly non-trivial. By contrast, in the latter case the maximal error is near the spike, varying up to two orders of magnitude over the range $2 \leq p \leq 5$ and evening out to a constant value at the tail. Illatively increments of 0.1 for p are hardly acceptable for p near 2: the relative error in $u(y)$ is only on the order of 10^{-2} . This estimate slowly improves for higher p . Increments of 0.01 in γ entail a relative error on the order of 10^{-3} through the range $1 \leq \gamma < 2$.

3. CONCLUSION

Replacement of a boundary condition with an asymptotics based tail condition is not unheard of (in [10] a conceptually similar procedure is described), however this is the first study of its kind showing that implementing the tail condition over a surprisingly large part of the computational domain markedly improves the solution

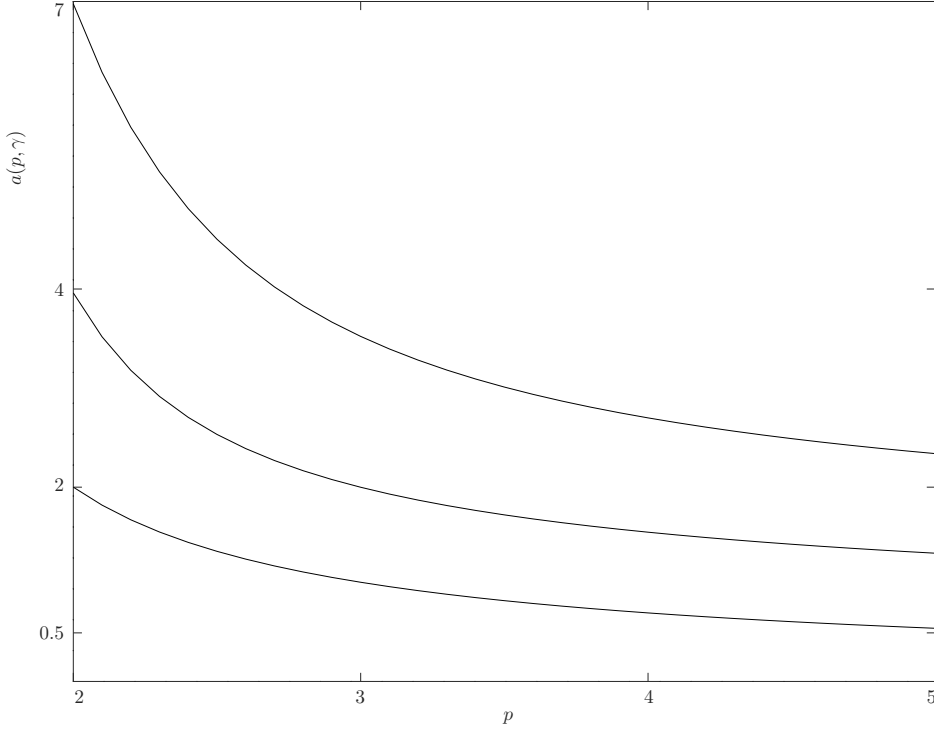


FIGURE 10. Tail constant $a(p, \gamma)$ for $\gamma = 1, 1.5, 1.95$ respectively from bottom curve to top.

accuracy; devising an optimisation procedure to determine the best implementation point; and establishing that tracking a derived quantity of interest yields a smooth dependence of all concomitant properties on the equation parameters. The approach is applicable to boundary value problems on infinite domains, where the sought function is characterised by a slow decay. An example problem was chosen from a wide class of equations with a two-dimensional parameter space, where one parameter controls non-linearity and the other governs the tail shape, allowing for both algebraic (slow) and exponential (fast) decay. It was shown that when the former problem is solved by the same means as the latter, the relative error incurred is dismayingly large – up to the order of unity, furthermore by far not confined to the boundary region (figure 1). The devised method allows to reduce the error magnitude by up to three orders and make it uniform throughout the domain (figure 6), a testament to the method’s merit, bearing in mind that the discrete problem solved numerically only approximates the desired solution at the limit $\epsilon \rightarrow 0$ and $D \rightarrow \infty$.

Since the fractional Laplacian operator $-(-\Delta)^{\gamma/2}$ had been first used decades ago to describe a Lévy flights dispersion with $1 \leq \gamma < 2$, several arguments were voiced for the unphysical behaviour thereof, the most prominent being that in contrast to the case $\gamma = 2$ the concomitant random walk probability density lacked a second spatial moment. This directly corresponds to the fact that at the limit $\gamma \rightarrow 2^-$ the algebraic tail would never approach the rate of exponential decay known for $\gamma = 2$. As a corollary this study obtained new numerical results in support of the physicality of Lévy flights as a dispersion model: (a) proper limit of the ground state peak at $\gamma \rightarrow 2$ approaching the normal value of $\frac{3}{2}$; (b) monotonic dependence of the tail decay constant and ground state peak when $1 \leq \gamma < 2$ and $2 \leq p \leq 5$. Albeit a “heavy” tail indicates that a particle is allowed to move infinitely far from its initial point in finite time – an ungainsayable problem deemed more

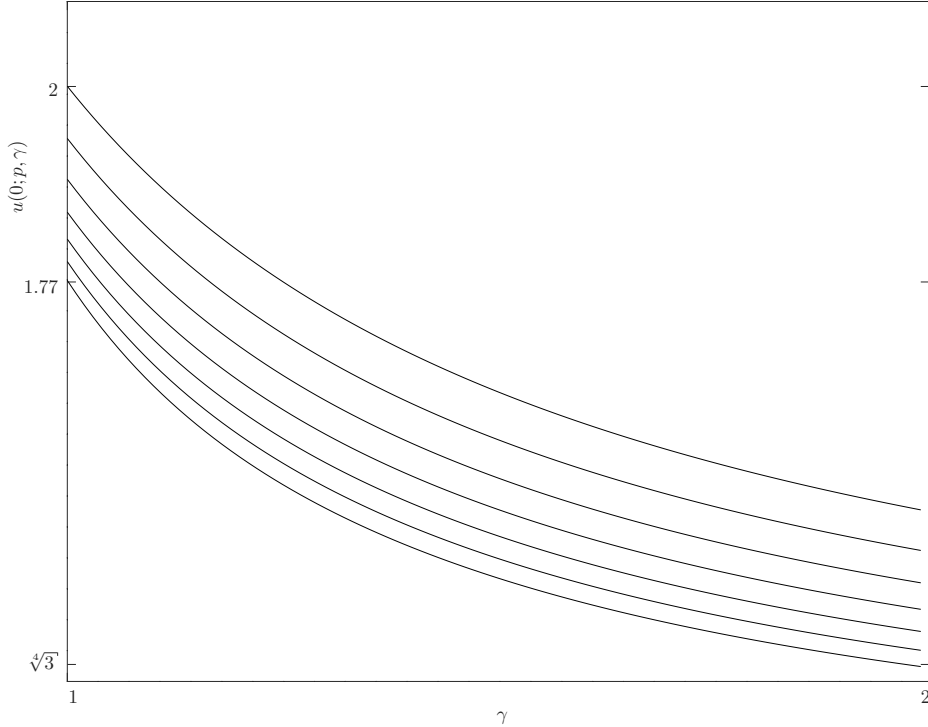


FIGURE 11. Spike peak $u(0; p, \gamma)$ for evenly spaced values $2 \leq p \leq 5$ in ascending order $2 \nearrow 5$ from top curve to bottom.

striking than the implied infinite velocity a particle acquires subject to Fickian diffusion, a proper limit in the ground state peak means that the highest concentration and its location are continuous between Lévy flights and Fickian diffusion. Non-monotonicity of derived or global properties for anomalous diffusion operators often forms a powerful argument of their non-physicality. Here the opposite was shown for Lévy flights.

In summary, a simplistic implementation of boundary condition for functions with slowly decaying tails is bound to affect the attained accuracy throughout the domain, begetting an error grossly exceeding the estimate associated with the numerical scheme chosen for the solution. The proposed method is generic and versatile, allowing to control the error whilst using well established solution schemes.

Acknowledgements. The authors thereby acknowledge the Canada Foundation for Innovation grant # 35174 that supported the computational cluster used to complete this study (YN) and partial funding by NSERC Undergraduate Student Research Award 521927–2018 (KB).

APPENDIX A NUMERICAL SCHEME PARAMETERS

All common parameters used to obtain the results reported herein are listed in table 1.

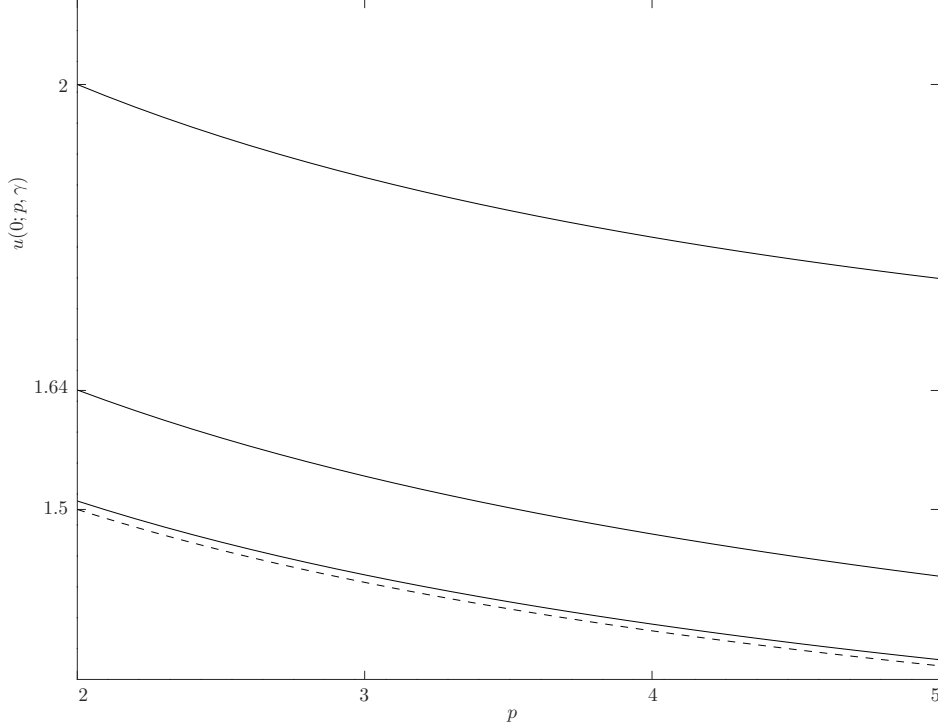


FIGURE 12. Spike peak $u(0; p, \gamma)$ for $2 \leq p \leq 5$ and $\gamma = 1, 1.5, 1.95$ (solid, respectively from top curve to bottom) and $\gamma = 2$ (dashed, regular diffusion, equation (3a)).

parameter	symbol	value
activator diffusion coefficient	ϵ	0.01
inhibitor diffusion coefficient	D	20000
reaction time constant	τ_o	0.001
number of mesh points	N	262144
Euler time step	δt	0.01
solution domain		$(-2\pi/\epsilon, 2\pi/\epsilon)$

TABLE 1. Numerical scheme parameters common to all computations

APPENDIX B INTEGRALS OF $u(y)$

The integral $b(p, \gamma) = \int_{-\infty}^{\infty} u^m dy$, $m > 0$, is useful in problems involving the homoclinic or ground state, as is the ratio $f(p, \gamma) = \int_{-\infty}^{\infty} u^{p+1} dy / \int_{-\infty}^{\infty} u'^2 dy$ [11, 12, 18]. The dependence $f(p, 2) = \frac{2(p+1)}{p-1}$ was formerly

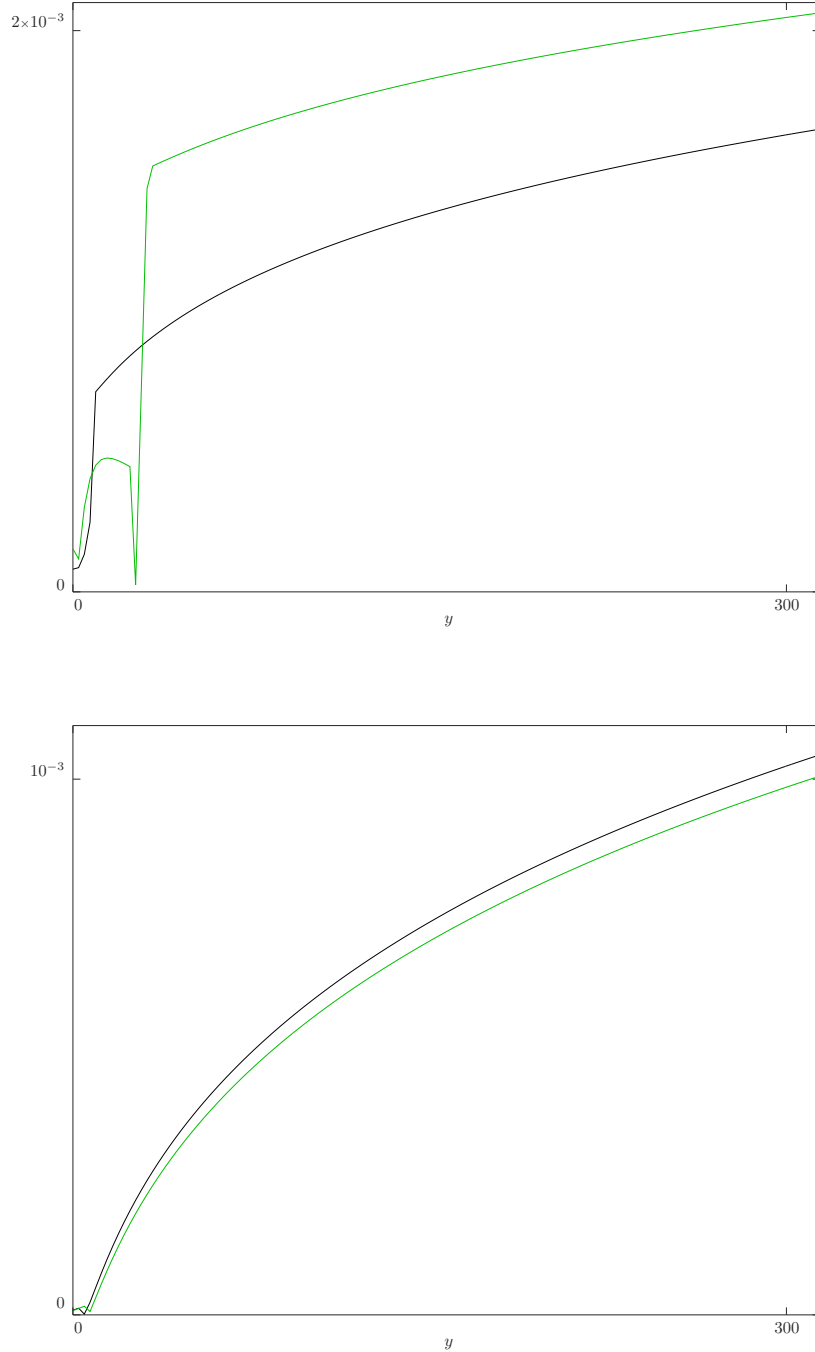


FIGURE 13. Relative error of interpolated and numerically solved ground states $\left| \frac{u(y; p, \gamma_1) + u(y; p, \gamma_2)}{2u(y; p, (\gamma_1 + \gamma_2)/2)} - 1 \right|$ for $p = 2$ (black) and $p = 5$ (grey/green). Top panel: $\gamma_1 = 1.04$, $\gamma_2 = 1.06$. Bottom panel: $\gamma_1 = 1.94$, $\gamma_2 = 1.96$.

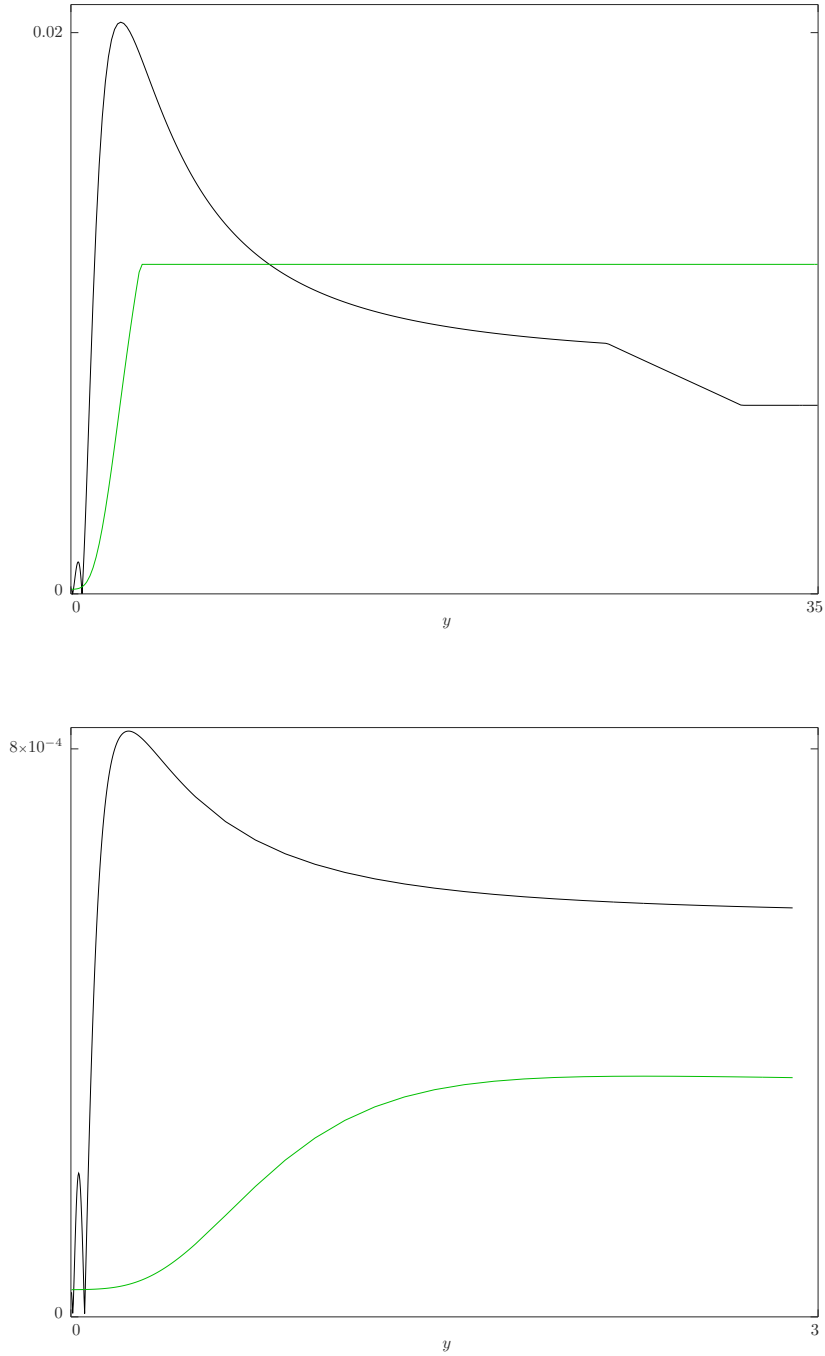


FIGURE 14. Relative error of interpolated and numerically solved ground states $\left| \frac{u(y; p_1, \gamma) + u(y; p_2, \gamma)}{2u(y; (p_1 + p_2)/2, \gamma)} - 1 \right|$ for $\gamma = 1$ (black) and $\gamma = 1.95$ (grey/green).
 Top panel: $p_1 = 2, p_2 = 2.2$. Bottom panel: $p_1 = 4.8, p_2 = 5$.

calculated as a ratio [12]. Both b and f are computable through the beta functions for $\gamma = 2$ with arbitrary p and $p = 2$, $\gamma = 1$. The beta function is defined as

$$B(\mu, \nu) = \int_0^1 t^{\mu-1} (1-t)^{\nu-1} dt. \quad (11a)$$

The following identities hold by the indicated transformation of the integration variable:

$$t \mapsto 1-t: \quad B(\mu, \nu) = B(\nu, \mu), \quad (11b)$$

$$t \mapsto t^2 \mapsto \sin t: \quad B(\mu, \nu) = 2 \int_0^{\pi/2} \sin^{2\mu-1} t \cos^{2\nu-1} t dt, \quad (11c)$$

$$t \mapsto \frac{1-t}{t} \mapsto t^2 \mapsto \sinh t: \quad 2 \int_0^\infty \sinh^{2\mu-1} t \cosh^{1-2(\mu+\nu)} t dt, \quad (11d)$$

where in the latter (11b) was used between the first and second transformations. With (11d) and (3a)

$$b(p, 2) = \frac{4}{p-1} \left(\frac{p+1}{2} \right)^{m/(p-1)} \int_0^\infty \cosh^{-2m/(p-1)} y dy = \frac{2}{p-1} \left(\frac{p+1}{2} \right)^{m/(p-1)} B\left(\frac{1}{2}, \frac{m}{p-1} \right). \quad (12a)$$

With (11c) and (3b)

$$b(2, 1) = 2^m \int_{-\infty}^\infty \frac{dy}{(1+y^2)^m} = 2^{m+1} \int_0^{\pi/2} \cos^{2(m-1)} y dy = 2^m B\left(\frac{1}{2}, m - \frac{1}{2} \right), \quad (12b)$$

where the second integral is obtained by changing the integration variable $y \mapsto \tan y$. The numerator in $f(2, 1)$ is then $\int_{-\infty}^\infty u^3 dy = 8B\left(\frac{1}{2}, \frac{5}{2} \right)$. The denominator gives $16 \int_{-\infty}^\infty \frac{y^2 dy}{(1+y^2)^4} = \frac{8}{3} \int_{-\infty}^\infty \frac{dy}{(1+y^2)^3} = \frac{8}{3} B\left(\frac{1}{2}, \frac{5}{2} \right)$, where the first equality follows from integration by parts and the second by (12b) with $m = 3$. Thus

$$f(2, 1) = 3. \quad (12c)$$

REFERENCES

- [1] B Baeumer, M Kovács, and M M Meerschaert. Fractional reproduction-dispersal equations and heavy tail dispersal kernels. *Bulletin Math. Bio.*, 69:2281–2297, 2007.
- [2] E Bakalis, S Höfner, and A Venturini. Crossover of two power laws in the anomalous diffusion of a two lipid membrane. *J. Chem. Phys.*, 142:215102, 2015.
- [3] B Barrios, E Colorado, A de Pablo, and U Sánchez. On some critical problems for the fractional Laplacian operator. *J. Diff. Eq.*, 252:6133–6162, 2012.
- [4] P Biler, T Funaki, and W A Woyczynski. Fractal Burgers equations. *J. Diff. Eq.*, 148:9–46, 1998.
- [5] C Brändle, E Colorado, A de Pablo, and U Sánchez. A concave–convex elliptic problem involving the fractional Laplacian. *Proc. Royal Soc. Edinburgh Section A: Mathematics*, 143:39–71, 2013.
- [6] D del Castillo-Negrete. Truncation effects in superdiffusive front propagation with Lévy flights. *Phys. Rev. E: Stat. Nonlin. Soft Matter Phys.*, 79:031120, 2009.
- [7] D Elliot. An asymptotic analysis of two algorithms for certain Hadamard finite-part integrals. *IAM J. Num. Analysis*, 13:445–462, 1993.
- [8] R L Frank and E Lenzmann. Uniqueness and nondegeneracy of ground states for $(-\Delta)^s Q + Q - Q^{\alpha+1} = 0$ in \mathbb{R} . *Acta Math.*, 210:261–318, 2013.

- [9] R L Frank, E Lenzmann, and L Silvestre. Uniqueness of radial solutions for the fractional Laplacian. *Comm. Pure and Appl. Math.*, 69:1, 2016.
- [10] C Froese. Numerical solution of the Hartree-Fock equations. *Canadian J. Phys.*, 41:1895–1910, 1963.
- [11] D Iron and M J Ward. The dynamics of multi-spike solutions to the one-dimensional Gierer-Meinhardt model. *SIAM J. Appl. Math.*, 109:229–264, 2002.
- [12] D Iron, M J Ward, and J Wei. The stability of spike solutions to the one-dimensional Gierer-Meinhardt model. *Physica D*, 150:25–62, 2001.
- [13] R Klages, G Radons, and I M Sokolov. *Anomalous transport: foundations and applications*. Wiley-VCH, Weinheim, 2008.
- [14] M Kohlbecker, S W Wheatcraft, and M M Meerschaert. Heavy-tailed log hydraulic conductivity distributions imply heavy-tailed log velocity distributions. *Water Resources Research*, 42:W04411, 2006.
- [15] F Liu, V Anh, and I Turner. Numerical solution of the space fractional Fokker-Planck equation. *J. Comp. Appl. Math.*, 166:209–219, 2004.
- [16] V E Lynch, B A Carreras, D del-Castillo-Negrete, K M Ferreira-Mejias, and H R Hicks. Numerical methods for the solution of partial differential equations of fractional order. *J. Comput. Phys.*, 192:406–421, 2003.
- [17] M M Meerschaert and C Tadjeran. Finite difference approximations for fractional advection – dispersion flow equations. *J. Comput. Appl. Math.*, 172:65–77, 2004.
- [18] Y Nec. Spike-type solutions to one dimensional Gierer-Meinhardt model with Lévy flights. *Stud. Appl. Math.*, 129:272–299, 2012.
- [19] K B Oldham and J Spanier. *Fractional Calculus*. Academic Press, New York, 1974.
- [20] I Podlubny. *Fractional differential equations*. Academic Press, 1998.
- [21] X Ros-Oton and J Serra. The Pohozaev identity for the fractional Laplacian. *Arch. Rational Mech. Anal.*, 213:587–628, 2014.
- [22] T Sandev, A Iomin, H Kantz, R Metzler, and A Chechkin. Comb model with slow and ultraslow diffusion. *Math. Model. Nat. Phenom.*, 11:18–33, 2016.
- [23] V A Volpert, Y Nec, and A A Nepomnyashchy. Fronts in anomalous diffusion – reaction systems. *Phil. Trans. R. Soc. A*, 371:20120179, 2013.